

# NUMERICAL SIMULATION OF THE LIQUID MOTION THROUGH HYDRAULIC RESISTANCES OF CONVERGENT AND DIVERGENT TYPE

Iosif Anton<sup>1</sup> Eleș Gabriel<sup>2</sup> Borza Ioan<sup>3</sup>

**Abstract** – This paper presents a numerical solving method for the axial-symmetrical flow of the inviscid and incompressible liquid through local hydraulic resistances of convergent or divergent type, using the Finit Element Method. The following elements were determined: the hydrodynamic field, the velocity and pressure distributions along the the streamline which coresponds to the solid boundary that delimitates the liquid's motion. **Keywords:** Finite elements, velocity potential, stream function,

## 1. INTRODUCTION

The use of modern computers has allowed the introduction of numerical experiment and the researcher has managed to create a synthesis between the analytical thought and the experimental one, for solving complex problems. Thus, one of the main scientific models of knowing the continual environments is the on based on discrete approximation. This model consists of decomposing a continual analysis domain in a finite number of discrete elements. In this case the approximation of the whole is accomplished by the ensemble of all of the composing elements. To simplify the application of the Finite Element Method (FEM), the stream function  $\psi$  or the velocity potential  $\phi$  will be used as auxiliary variables. This paper presents just how to integrate the Stokes equation in the flow function using FEM, mentioning the limit conditions and the recovery of the primitive variables like velocities and determining the pressures field by writing a Bernoulli theorem.

## 2. INTEGRATION WITH FEM OF THE STOKES EQUATION IN A STREAM FUNCTION

The axial-symmetrical motion, due to the fact that  $\frac{\partial v}{\partial \theta} = 0$ , imposes a cylindrical coordinates system

$(r, \theta, z)$ . Taking into account that the liquid is considered incompressible and the  $\vec{v}$  velocity components have the following expressions [1], [6], [13]:

$$v_z = \frac{1}{r} \frac{\partial \psi}{\partial r} \quad ; \quad v_r = -\frac{1}{r} \frac{\partial \psi}{\partial z} \quad (1)$$

The result is:

$$\frac{\partial^2 \psi}{\partial z^2} + \frac{\partial^2 \psi}{\partial r^2} - \frac{1}{r} \frac{\partial \psi}{\partial r} = 0 \quad (2)$$

known as the Stokes equations in the stream function  $\psi$ . Because the motion is considered to be a potential one, meaning  $\vec{v} = \nabla \phi$ , the velocity can be writen as:

$$v_z = \frac{\partial \phi}{\partial z} \quad ; \quad v_r = \frac{\partial \phi}{\partial r} \quad (3)$$

In order to make the problem a general one it is natural to study it under a dimensionless form and thus we will be making the following variable and function changes:

$$z^* = z L_{ax}^{-1} \quad r^* = r L_{ax}^{-1} \quad ; \quad \psi^* = 2\pi Q^{-1} \psi \quad (4)$$

$Q$  - flow rate,  $L_{ax}$  - is the axial extent of the analysis domain  $\Omega$ , that has the boundary  $\Gamma$ . This change will lead to the Stokes equation written under a dimensionless form in the stream function:

$$\frac{\partial^2 \psi^*}{\partial z^{*2}} + \frac{\partial^2 \psi^*}{\partial r^{*2}} - \frac{1}{r^*} \frac{\partial \psi^*}{\partial r^*} = 0 \quad (5)$$

The dimensionless velocities are:

$$v_{z^*}^* = \frac{1}{r^*} \frac{\partial \psi^*}{\partial r^*} \quad ; \quad v_{r^*}^* = -\frac{1}{r^*} \frac{\partial \psi^*}{\partial z^*} \quad (6)$$

and the connection between them is:

$$v_{z^*}^* = 2\pi L_{ax}^2 Q^{-1} v_z \quad ; \quad v_{r^*}^* = 2\pi L_{ax}^2 Q^{-1} v_r \quad (7)$$

Equation (5) on the  $\Omega^*$  domain with  $\Gamma^*$  as its boundary, complies with the Dirichlet and Neumann

<sup>1,2,3</sup> Politehnica University of Timisoara, Traian Lalescu Street, no.2A, 300223, Romania, [anton.iosif@ct.upt.ro](mailto:anton.iosif@ct.upt.ro)  
[eles.gabriel@ct.upt.com](mailto:eles.gabriel@ct.upt.com), [ioan.borza@ct.upt.ro](mailto:ioan.borza@ct.upt.ro)

limit conditions, and the function  $\psi^*$  can be globally approximated on  $\Omega^*$  as follows:

$$\psi^* = a_\alpha^* \psi_\alpha^* \quad \alpha = 1, G \quad (8)$$

where,  $G$  is the number of nodes on  $\Omega^*$ , and  $a_\alpha^*$ ,  $\psi_\alpha^*$  are the global interpolation functions and the global values of  $\psi^*$  in the global node  $\alpha$ .

Applying Galerkin's method we have:

$$\int_{\Omega^*} \left( \frac{\partial^2 \psi^*}{\partial z^{*2}} + \frac{\partial^2 \psi^*}{\partial r^{*2}} - \frac{1}{r^*} \frac{\partial \psi^*}{\partial r^*} \right) a_\alpha^* d\Omega^* = 0 \quad (9)$$

which integrated by parts leads to the next global linear system [8],[13]:

$$D_{\alpha\beta}^* \psi_\beta^* = F_\alpha^* \quad (10)$$

in which:

$$D_{\alpha\beta}^* = \int_{\Omega^*} \frac{\partial a_\alpha^*}{\partial z^*} \frac{\partial a_\beta^*}{\partial z^*} r^* d\theta dr^* dz^* + \int_{\Omega^*} \frac{\partial a_\alpha^*}{\partial r^*} \frac{\partial a_\beta^*}{\partial r^*} r^* d\theta dr^* dz^* + 2 \int_{\Omega^*} a_\alpha^* \frac{\partial a_\beta^*}{\partial r^*} d\theta dr^* dz^* \quad (11)$$

$$F_\alpha^* = \int_{\Gamma^*} \frac{\partial \psi^*}{\partial z^*} a_\alpha^* r^* d\theta dr^* + \int_{\Gamma^*} \frac{\partial \psi^*}{\partial r^*} a_\alpha^* r^* d\theta dz^* \quad (12)$$

in which  $a_\alpha^*$  are the global approximation functions on the boundary  $\Gamma^*$ . If we establish a discrete process of  $\Omega^*$ , noted  $\Omega^{*e}$  and having the boundary  $\Gamma^{*e}$ , consisting of  $E$  finite elements, that the function  $\psi^*$  can be approximated locally on  $\Omega^{*e}$ , as follows:

$$\psi^{*e} = a_N^{*e} \psi_N^{*e} \quad N = 1, F \quad (13)$$

in which  $a_N^{*e}$  are the local interpolation functions,  $\psi_N^{*e}$  is the value  $\psi^*$  in node  $N$  of  $\Omega^{*e}$ , and  $F$  is the total number of local nodes of the finite element. If we apply the Galerkin method in the same way and also use the integration by parts we will obtain the following local linear system:

$$D_{NM}^{*e} \psi_M^{*e} = F_N^{*e} \quad N, M = 1, F \quad (14)$$

in which  $D_{NM}^{*e}$  coefficients and the local free terms  $F_N^{*e}$  have the expressions:

$$D_{NM}^{*e} = \int_{\Omega^{*e}} \frac{\partial a_N^{*e}}{\partial z^*} \frac{\partial a_M^{*e}}{\partial z^*} d\Omega^{*e} + \int_{\Omega^{*e}} \frac{\partial a_N^{*e}}{\partial r^*} \frac{\partial a_M^{*e}}{\partial r^*} d\Omega^{*e} + 2 \int_{\Omega^{*e}} \frac{a_N^{*e}}{r^*} \frac{\partial a_M^{*e}}{\partial r^*} d\Omega^{*e} \quad (15)$$

$$F_N^{*e} = \int_{\Gamma^{*e}} \frac{\partial \psi^{*e}}{\partial z^*} \cos(n^*, z^*) a_N^{*e} d\Gamma^{*e} + \int_{\Gamma^{*e}} \frac{\partial \psi^{*e}}{\partial r^*} \cos(n^*, r^*) a_N^{*e} d\Gamma^{*e} \quad (16)$$

If we take account into the analysis domain in the form of finite isoparametric discrete elements, as presented in figure 1, the  $D_{NM}^{*e}$  coefficients are numerically evaluated using a quadrature Gauss formula to comply with [1], [8],[9], [13]:

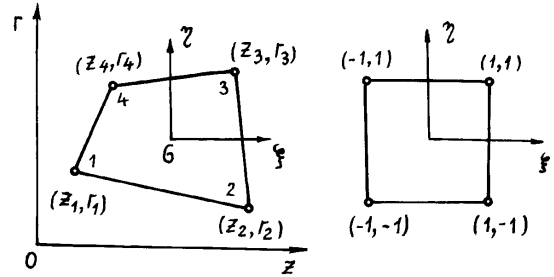


Figure1 Global and  $\xi$  - natural coordinates for linear quadrilateral elements

$$D_{NM}^{*e} = 32^{-1} \sum_{i=1}^m \sum_{j=1}^m w_i w_j f(\xi_i, \eta_j) \quad (17)$$

in which  $m$  represents the number of Gauss points of  $\xi_i$  and  $\eta_i$  coordinates on the finite element, and  $w_i$ ,  $w_j$  are the ponderate functions. The free terms  $F_N^{*e}$  are equal to zero in the case of a velocities field orthogonal on the entry boundary of the analysis domain. Moving from local values to global ones is done with the Boolean matrixes [8], [13]:

$$\psi_\alpha^* = \sum_{e=1}^E \Delta_{N\alpha}^e \psi_N^{*e} \quad D_{\alpha\beta}^* = \sum_{e=1}^E D_{NM}^{*e} \Delta_{N\alpha}^e \Delta_{M\beta}^e \quad F_\alpha^* = \sum_{e=1}^E F_N^{*e} \Delta_{N\alpha}^e \quad (18)$$

The velocity components on the finite element in the case in which the velocity is calculated in then gravity centre of the finite element, is determined with expressions [8], [7]:

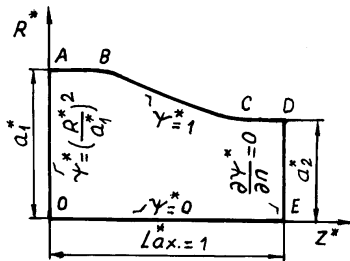
$$\bar{v} = \frac{v^*}{v^{*AB}} \quad ; \quad \bar{p} = 1 - \bar{v}^{*2} \quad (20)$$

in with  $v^{*AB}$  is the entry boundary velocity of the domain. The calculus for the potential function is done from entry in the domain to its exit, using the following written relation between points  $M_i$  and  $M_j$ , as follows:

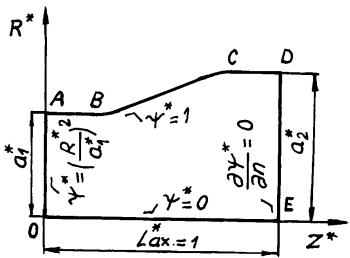
$$\varphi_{M_i}^* = \varphi_{M_j}^* + \int_{M_i}^{M_j} v_z^* dz^* + \int_{M_i}^{M_j} v_r^* dr^* \quad (21)$$

### 3. NUMERICAL RESULTS

The numerical simulation in the case of potential axial-symmetrical motion considering the ideal and incompressible liquid, was done with FEM in the presence of local hydraulic resistances of convergent or divergent type. The hydraulic resistances suggested for the flow simulation have the same geometry except for the convergent regime where the convergent exit is inversed with the divergent entry. Figure 2 presents the analysis domain and the limit conditions. Because the domain is axial-symmetrical, the flow study requires just the axial semiplane superior to the symmetry axis.



a) Convergent regime



b) Divergent regime

Figure 2 Analysis domain and limit conditions for dimensionless status

We have to state that for the convergent regime we have a drop in the dimension of the section from  $D_1=50$  mm  $D_2=26$  mm, and the axial extent is  $L_{ax}=160$  mm. In the case of the divergent regime we have a growth of the section  $D_2$  to  $D_1$  and the same value  $L_{ax}$ . In the case of dimensionless status we must state the following values:  $a_1^* = 0.15625$ ,  $a_2^* = 0.08125$ ,

$AB = CD = 0.25$ , and the equations that describe the solid boundary BC, for  $Z^* \in [0.25, 0.75]$ , are:

$$R^* = 0.14037 + 0.28088 Z^* - 1.0643 Z^{*2} + 0.7796 Z^{*3} \quad \text{convergent} \quad (22)$$

$$R^* = 0.13654 - 0.49108 Z^* + 1.2745 Z^{*2} - 0.7796 Z^{*3} \quad \text{divergent} \quad (23)$$

Figures 3 and 4 present the discrete analysis domain in linear finite elements shaped as a square also stating a global node numbering system. The analysis domain for both the convergent and divergent regimes is discrete into a number of E=200 finite elements and G=246 global nodes. The hydrodynamic field for both cases is presented in figures 5 and 6.

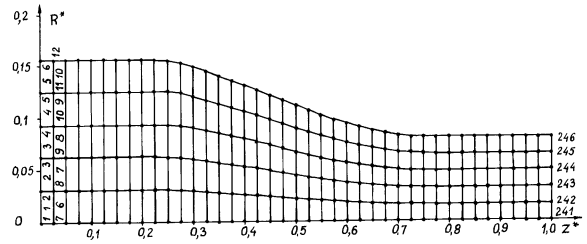


Figure 3 Discretization of the analysis domain for the convergent regime

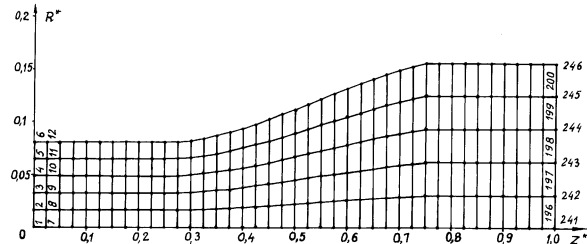


Figure 4 Discretization of the analysis domain for the divergent regime

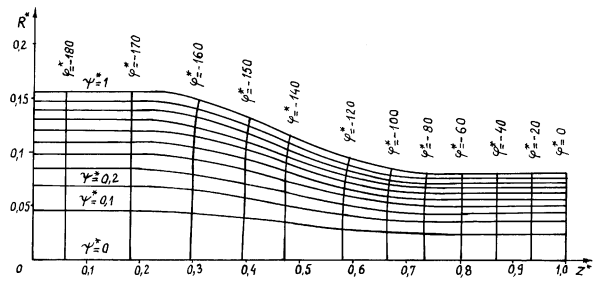


Figure 5 Hydrodynamic field in the convergent regime

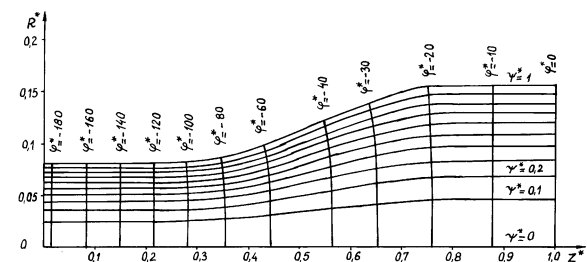


Figure 6 Hydrodynamic field in the divergent regime

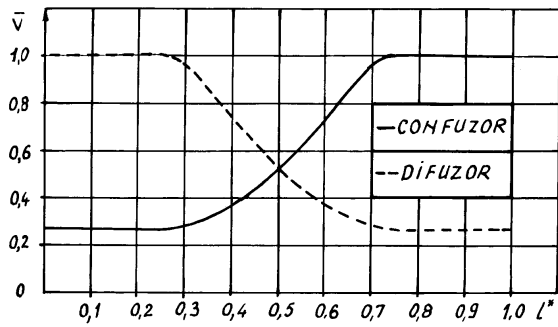


Figure 7 Velocities distributions in the convergent and divergent regime

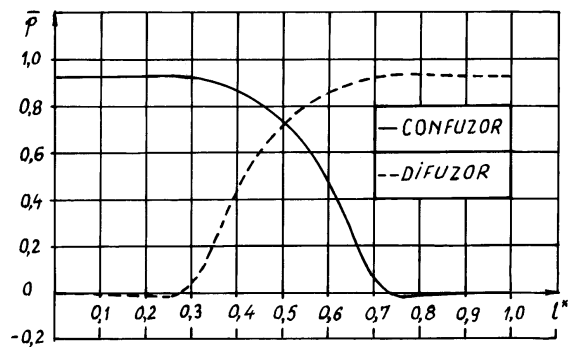


Figure 8 Pressures distributions in the convergent and divergent regime

Figures 7 and 8 present the velocities and pressures distributions corresponding to the solid boundary ABCD, when  $\psi^* = 1$  in the convergent case, respectively the divergent case. To compare the velocities and pressures distributions in the convergent case means to turn velocity  $v^*$  into a dimensionless one  $v^{*DE}$  which exits the domain.

#### 4. CONCLUSIONS

The potential axial-symmetrical motion has been simulated for the local hydraulic resistances of the convergent and divergent type, in the hypothesis of the inviscid and incompressible liquid, with the help of Finite Element Method.

From the velocities and pressures on the entry boundary in the convergent regime are equal to those at the exit in the divergent regime.

Knowing the equations that define parts of the solid boundary leads to eliminating the angular points that would appear on them, if the boundary parts are traced through points, and also eliminating the leaps from velocities and pressures field.

The programme PSIELFAS is flexible and allows a change in the solid boundary portions so that we don't have sudden variations in the velocities and pressures field.

Accomplishing a smooth solid boundary and certain velocities and pressures distributions will lead to an optimized flow domain.

#### REFERENCES

- [1] Anton I., Cămpian V., Carte I., *Hidrodinamica turbinelor bulb și a turbinelor pompe bulb*, Ed. Tehnică, București, 1988.
- [2] Banerjee P. K., *The Boundary Element Method in Engineering*, McGraw-Hill, London, 1992.
- [3] Brebbia C. A., *Boundary Element Techniques*, Springer-Verlag, Berlin, 1984.
- [4] Brătianu C., *Metode cu elemente finite în dinamica fluidelor*, Editura Academiei RSR, București, 1983.
- [5] Caius I., Homentcovschi D., Marcov N., Ncolau A., *Matematici clasice și moderne*, Editura Tehnică, București, 1983.
- [6] Carafoli E., Constantinescu V. N., *Dinamica fluidelor incompresibile*, Editura Academiei RSR, București, 1981.
- [7] Carte I. N., *Contribuții la studiul rețelelor de profile radial-axiale și utilizarea lor în proiectarea rotorilor turbinelor Francis*, Teză de doctorat, Timișoara, 1986.
- [8] Chung T. J., *Finite Element Analysis in Fluids Dynamics*, Mc Graw-Hills, New-York, 1978.
- [9] Connor J. J., Brebbia C. A., *Finite Element Techniques for Fluid Flow*, Newnes-Buterworths, London, 1976.
- [10] Davies A. J., *The Finite Element Method*, Clarendon Press, Oxford, 1980.
- [11] Desai C. S., *Elementary Finite Element Method*, Prentice-Hall, New Jersey, 1979.
- [12] Gârbea D., *Analiza cu elemente finite*, Editura Tehnică, București, 1990.
- [13] Iosif A., *Mașini hidraulice radial-axiale reversibile*, Teză de doctorat, Timișoara, 1999.
- [14] Iosif A., *Determining the hydrodynamic field when the liquid flow passes through the bars of a raking screen*, Buletinul Științific al Universității "Politehnica" din Timișoara, Tom 46 (60), fasc. 2, 2001, pg. 45÷52.
- [15] Olariu V., Brătianu C., *Modelarea numerică cu elemente finite*, Editura Tehnică, București, 1986.
- [16] Reddy J. N., *An introduction to the Finite Element Method*, McGraw-Hill, New York, 1984.
- [17] Strang G., Fix G., *An analysis of the Finite Element Method*, Prentice -Hall, New Jersey, 1975.
- [18] Titus P., Gheorghiu C. I., *Metode element finit și aplicații*, Editura Academiei RSR, București, 1987.
- [19] Zienkiewicz O. C., *Finite Element Method*, McGraw-Hill, London, 1977.